Wind and Structures, Vol. 15, No. 4 (2012) 285-299
DOI: http://dx.doi.org/10.12989/was.2012.15.4.285

Structural monitoring of a wind turbine steel tower – Part I: system description and calibration

C. Rebelo*[1], M. Veljkovic[2], L. Simões da Silva[1], R. Simões[1] and J. Henriques[1]

[1]*ISISE, Civil Engineering Department, University of Coimbra, Rua Luís Reis Santos, Coimbra, Portugal*
[2]*Luleå University of Technology, SE-97187 Luleå, Sweden*

(Received March 8, 2011, Revised August 30. 2011, Accepted August 31, 2011)

Abstract. This paper describes the development and calibration of a structural monitoring system installed in a 80 meters high steel wind tower supporting a 2.1 MW turbine Wind Class III IEC2a erected in the central part of Portugal. The several signals are measured at four different levels and include accelerations, strains on the tower wall and inside the connection bolts, inclinations and temperature. In order to correlate measurements with the wind velocity and direction and with the turbine operational parameters the corresponding signals are obtained directly from the turbine own monitoring system and are incorporated in the developed system. Results from the system calibration, the structural identification and the initial period of data acquisition are presented in this paper.

Keywords: Wind tower; steel; monitoring; wind loading; modal identification; stresses; dynamic response

1. Introduction

Within the research project *HISTWIN* (High strength steel towers for wind turbines) (Veljkovic *et al*. 2010a) which aims to ensure the competitiveness of the next generation of steel towers for wind turbines, a comprehensive experimental program was planned and carried out. It includes experimental laboratory tests of a new type of friction connection between the tower segments and the structural monitoring of a conventional tubular steel wind tower. In this project various aspects of the behaviour of the steel towers are addressed with particular emphasis on the behaviour of the connections between the tower segments and on the fatigue problems raised by the type of connection (Veljkovic *et al*. 2010b, 2011, CEN 2005). Besides the specific objectives of the research project, results obtained from the structural monitoring of the tower reflecting the real behaviour may be used to estimate calculation model uncertainties. Therefore, it should be possible to prevent, more realistically, damage during extreme events, as such reported by Chou and Tu (2011).

This paper presents the concept, the calibration and structural identification and initial results of the experimental program concerning the on-site long-term monitoring performed on a steel wind tower. Results from the one and half years long monitoring will be presented in a companion paper (Rebelo *et al*. 2011). The objectives established for this monitoring were the acquisition and processing of data concerning the dynamic behaviour of the tower during operation and the

* Corresponding author, Assistant Professor, E-mail: crebelo@dec.uc.pt

characterization of internal stresses and related internal forces acting on the shell and on the connection at different tower levels. The dynamic response for different wind speeds and the estimation of load fatigue spectra are also specific objectives (Adams *et al*. 2011, Hau 2006, Burton 2001). This should allow a better understanding of the structural performance, concerning in particular the bolted joints and the behaviour of the thin walled section in the vicinity of those joints.

The physical quantities under observation are the strains on the inner surface of the steel conical shell and inside some of the bolts used in the connections, the accelerations at various levels, the inclinations in the upper part of the tower, the surface temperature at a fixed level and several parameters related to the wind turbine operation.

Calibration tests on the monitoring system and measurements made during a monitoring period thereafter are used to present a set of results in this paper. During this period the signal recording was activated either manually or for wind speeds over 6 m/s. This limit was increased thereafter during regular monitoring to values of 12 m/s to 14 m/s. When started, the automatic recording of the signals lasts one hour before a new trigger event can restart the data recording.

2. Description of the wind tower

The wind turbine is a 2.1 MW turbine Wind Class III IEC2a and is mounted on a 80 metres high steel tower erected in the central part of Portugal. The structure of the tower (Fig. 1) is a free standing tube with varying diameter and wall thickness along the height. To enable transportation and assembling on the construction site the tower is divided in three segments with lengths 21770, 26620 and 27760 mm. The diameter varies between 2955 mm at the tower top and 4300 mm at the

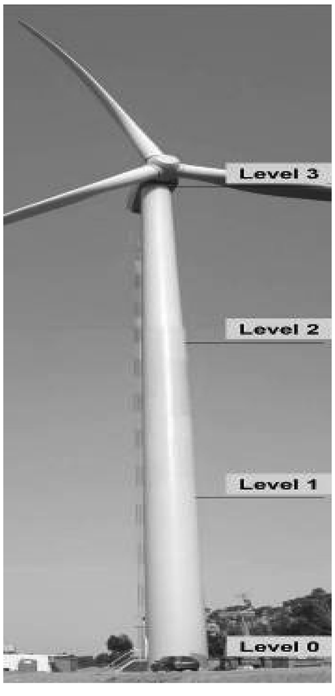

Fig. 1 Instrumented tower

tower bottom. The shell thickness varies between 12 and 30 mm at the same levels.

The instrumented tower is built in the usual configuration where the connection between tower segments is achieved using very stiff ring flanges welded to the segments' top and bottom plates using M36 e M42 class 10.9 bolts for assembling. The maintenance plan of the tower specifies tightening torques for the bolts of 2800 Nm and 4500 Nm, respectively.

According to the tower design plans the tube cross section properties along the height are calculated and given in Table 1. Level zero is at the tower bottom and level three is just below the nacelle. Intermediate levels coincide with internal work platforms and tower segment connections.

An important issue is the dimensional fabrication tolerances of the ring flanges used to connect the tower segments. Imperfections are responsible for the loss of contact between some parts of the flanges leading to water infiltrations and to low performance of the bolts which remain subjected to higher stress ranges. The fabrication tolerance limit for the 10 cm thick flange is 1.5 mm for the amplitude of the waviness and for the external-internal inclination of the ring surface. These tolerances are guaranteed by the tower manufacturer and no imperfections were detected during the visual inspection made to the tower during assembling and thereafter.

3. Measurement system

3.1 Type and location of sensors

Four types of signals are measured and recorded by the monitoring system, which are accelerations, strains, temperature and inclination (Dally 1993, Swartz 2010). Sensors and data loggers are placed at the defined four levels (see Fig. 1 and Table 1).

The acquisition of horizontal accelerations at different levels of the tower allows for the identification of the modal parameters and gives information about the evolution of the dynamic response during monitoring. The position and identification of the accelerometers at different levels are given in Table 2. A total of nine piezoelectric accelerometers are used of the type PCB393B04 with a dynamic frequency range of 0.1 Hz to 1000 Hz and a nominal sensitivity of 0.1 Volt/ms^{-2}.

Strains are measured on the inner surface of the shell on points distributed along the perimeter of the tube and inside 6 bolts per each assemble connections. The instrumented sections are located about two meters below the assembling joints and about six meters above the bottom joint (see Table 1). Gauge rosettes of type TML PFR-20-11 are used to measure shell strains in two orthogonal directions, vertical and horizontal, and in a 45º-direction (Fig. 2(a)). Gauges of type TML BTM-6C are used to measure bolt strains (Fig. 2(b)). A total of 96 strain channels are monitored, whose position and identification are given in Table 2.

Although not of decisive importance for the structural monitoring, because of the mild climate at the construction site, the inner temperature variation on the inner surface of the tower is monitored with four thermocouples of type K placed at level 2.

Two inclinometers of type TML-KB-5EB were placed at levels 2 and 3 to measure the inclination of the tower in two directions. This information is used to calibrate displacements obtained from the double integration of the accelerations and allows the estimation of the lateral displacements of the tower.

Table 1 Tube cross-section properties along the height

Height [m]	Diameter [m]	Thickness [m]	Inertia [m^4]	Levels for instrumentation
0.000	**4.300**	**0.030**	**0.9367**	**Connection Level 0**
2.000	4.276	0.030	0.9211	
3.082	4.257	0.030	0.9089	
5.412	4.215	0.030	0.8823	
5.802	**4.208**	**0.026**	**0.7608**	**Level 0**
7.789	4.173	0.026	0.7420	
9.302	4.147	0.027	0.7562	
11.502	4.108	0.024	0.6534	
12.582	4.089	0.023	0.6175	
15.172	4.043	0.022	0.5710	
17.362	4.004	0.022	0.5546	
17.972	**3.993**	**0.022**	**0.5500**	**Level 1**
19.752	**3.962**	**0.022**	**0.5373**	**Connection Level 1**
22.182	3.917	0.021	0.4956	
22.362	3.917	0.020	0.4720	
25.252	3.864	0.020	0.4531	
28.002	3.816	0.020	0.4364	
30.752	3.768	0.020	0.4202	
31.982	3.746	0.019	0.3922	
34.382	3.704	0.019	0.3792	
36.252	3.671	0.019	0.3691	
39.002	3.622	0.018	0.3359	
41.752	3.574	0.018	0.3227	
43.982	3.535	0.017	0.2949	
44.592	**3.524**	**0.017**	**0.2922**	**Level 2**
46.382	**3.492**	**0.017**	**0.2843**	**Connection Level 2**
48.817	3.448	0.016	0.2576	
48.967	3.448	0.015	0.2415	
51.552	3.400	0.015	0.2315	
53.812	3.360	0.015	0.2234	
55.502	3.330	0.014	0.2030	
58.252	3.280	0.014	0.1940	
58.622	3.277	0.013	0.1797	
61.022	3.231	0.013	0.1722	
63.752	3.182	0.013	0.1645	
65.842	3.144	0.013	0.1587	
66.502	3.133	0.012	0.1449	
69.252	3.083	0.012	0.1381	
71.152	**3.049**	**0.012**	**0.1336**	**Level 3**
72.002	3.034	0.012	0.1316	
73.082	3.015	0.012	0.1292	
75.492	2.971	0.014	0.1442	
75.640	2.955	0.018	0.1824	

Table 2 Sensors' location and identification

	Cross section at different levels	Sensors and locations
Level 3	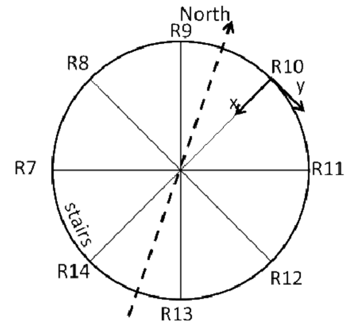	**Accelerometers:** positions R10-*x*, R10-*y*, R8-*x* (signals: L3AccX; L3AccY; L3AccT) **Strain gauges -** 1 rosette at each of the 8 locations along the inner perimeter of the section (signals: L3R7; L3R8; L3R9; L3R10; L3R11; L3R12; L3R13; L3R14) **Inclinometers –** R10-*x* and R10-*y* (signals: L3IncX; L3IncY) ***Section position and dimensions (mm):*** Height: 71152; Diameter:3049; Thickness: 12
Level 2	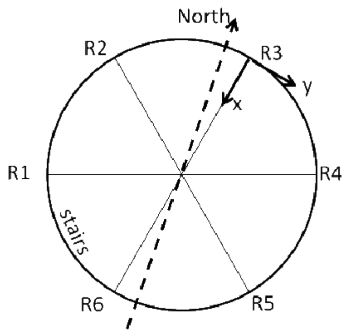	**Accelerometer:** R3-*x* and R3-*y* (signals: L2AccX; L2AccY) **Strain gauges -** 1 rosette at each of the 6 locations along the inner perimeter and 6 Strain gauge inside the bolts; (signals: L2R1; L2R2; L2R3; L2R4; L2R5; L2R6; L2B1; L2B2; L2B3; L2B4; L2B5; L2B6) **Temperature -** 4 Termocouples positions R1, R3 R4, R6 (signals: L3T1; L2T2; L2T3; L2T4) **Inclinometers –** R3-*x* and R3-*y* (signals: L2IncX; L2IncY) ***Section position and dimensions (mm):*** Height: 44592; Diameter:3524; Thickness: 17
Level 1	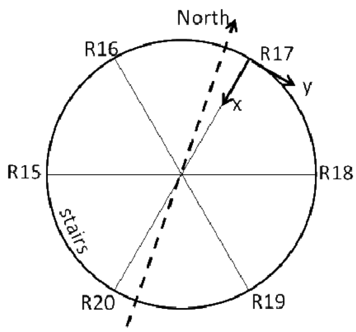	**Accelerometer:** R17-*y* and R17-*y* (signals: L1AccX; L2AccY) **Strain gauges -** 1 rosette at each of the 6 locations along the inner perimeter and 6 Strain gauge inside the bolts (signals: L1R15; L1R16; L1R17; L1R18; L1R19; L1R20; L1B1; L1B2; L1B3; L1B4; L1B5; L1B6) ***Section position and dimensions (mm):*** Height: 17972; Diameter:3993; Thickness: 22
Level 0	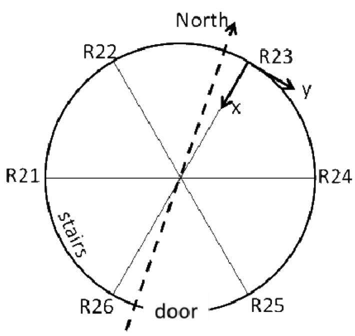	**Accelerometer:** R23-*y* and R23-*y* (signals: L0AccX; L0AccY) **Strain gauges -** 1 rosette at each of the 6 locations along the inner perimeter and 6 Strain gauge inside the bolts; (signals: L0R21; L0R22; L0R23; L0R24; L0R25; L0R26; L0B1; L0B2; L0B3; L0B4; L0B5; L0B6) ***Section position and dimensions (mm):*** Height: 5802; Diameter:4208; Thickness: 26

Initials for Signals' identification L(1)(2)(3)(4) (1) level number (2) Type of signal - R – strain gauge Rosette - Acc – accelerometer - B – starin gauge in bolt - Inc – inclinometer - Tmp – temperature	Location(see figures above) Strain gauge direction in rosettes V – vertical along tower axis H – horizontal along section perimeter D – diagonal e.g., **L2R21D:** **L**evel **2**, **R**osette **21**, strain gauge in Diagonal direction

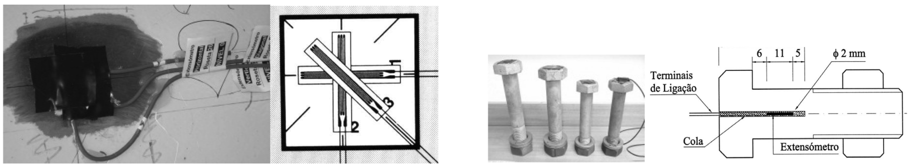

(a) (b)

Fig. 2 Details of strain gauges : (a) Strain rosettes on the inner side of the shell and (b) strain gauges inside the bolts

3.2 Data acquisition and transmission

The direct access to the information available in the monitoring system embedded in the turbine system running under the responsibility of the tower manufacturer was possible. Therefore, information is obtained concerning wind velocity, wind direction, turbine azimuth and rotor velocity and pitch angle. The signals are collected from the turbine system and included in the developed structural monitoring system for recording with the other signals.Data logging equipment suitable to perform dynamic measurements use to be more expensive than equipment suitable for data logging (quasi-)static signal. Therefore some decisions concerning the number of dynamic channels that could be measured had to be taken from the very beginning. Consequently, the use of available dynamic channels was given priority to accelerations and strains on the upper part of the tower where possibly higher frequencies coming from the rotor could influence the response.The data acquisition is performed using National Instruments (NI) equipment (Fig. 3). The data logger type NI cRio 9012 is able to digitalize dynamic data and is used for all acceleration sensors and for strain measurements at levels 2 and 3. Acquisition frequency rate of dynamic signals may be varied in the configuration data file of the acquisition software. Typically signals are recorded at a sampling rate of 100 Hz allowing unbiased spectral estimations of the measured signals up to 50 Hz. Data logger type NI cFP1808 is used to acquire signal from strain gauges at levels 0 and 1 using a lower rate of 2.5 Hz, which is the same rate used to digitalize the signals collected from the turbine. The lower sampling rate may lead to underestimate of the strain at this level. It is noted that both the first natural frequency of the tower and the loading frequency from the blade rotation are within the unbiased spectral range of 0 to 1.25 Hz. Therefore, most of the dynamic response is still assessed through this low acquisition rate. A computer application was developed in LabView (NI 2006) to synchronize the data loggers which are connected using TCP-IP communication protocols (Fig. 4). All measured data is recorded in a local database and a daily report is emailed to a remote system using a General Packet Radio Service (*GPRS*) based mobile data service. The software

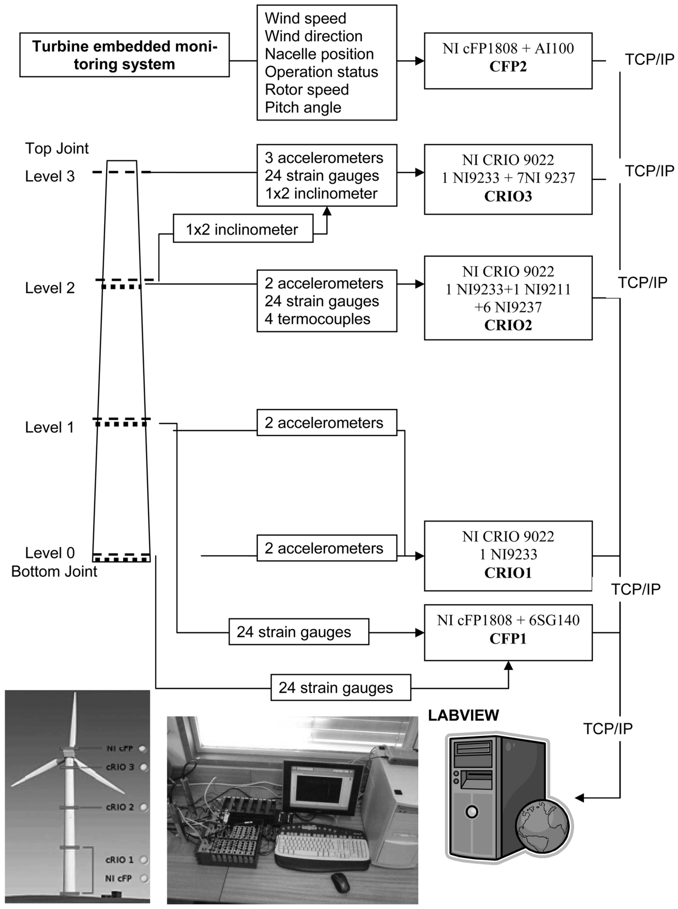

Fig. 3 Data logging and transmission inside the tower

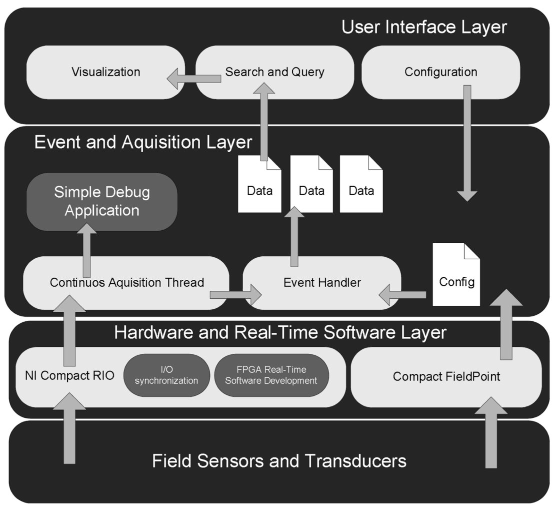

Fig. 4 Architecture of the LabView based computer application developed for synchronizing data loggers, signal decimation and recording

application uses triggering levels based on the wind velocity to perform automatic recording. Remote access to the system is possible for malfunction detection, software upgrading or manual start and stop of the acquisition system. Nevertheless this access is relatively slow due to the low speed *GPRS* transmission technology available on location.

4. System calibration

Calibration of the measurement system must allow the assessment of two different types of coefficients: i) those inherent to the conversion of electrical into physical quantities and ii) those related to the zeroing of the signal. The first type is sensor specific and will not be addressed here. The second type is important for the interpretation of the measured strains and is discussed below.

To interpret the strains obtained from the measurements, it is necessary to take into account that the measurement system was powered on after erection of tower and mounting of all the equipment. Therefore, the measured strains are not absolute values but relative to the moment of system initialization, i.e., these values only reproduce the time varying response under external wind action and internal operation related loading. Since the mean value over time should be zero when wind actions acting on the tower are zero and the turbine is in an idle position, the calibration of the measurement system should be ideally performed under these conditions. In practice, only measurements during very low wind speed and rotor in idle position are possible and were performed as a good approximation for zeroing the measurement system.

Fig. 5 schematically illustrates the absolute time dependent strain history obtained in a given measurement point during tower operation and its decomposition in several superposed components, either included or not in the measured values. The line showing the strain component due to time invariant self-weights cannot be measured because the data acquisition system was powered on after self-weight was acting. However it can be accurately estimated numerically from the components' self-weight. For instance, at the measurement points on the tower shell, the following compressive vertical stresses due to tower self-weight were computed: 3.56 and 2.69 MPa for levels 0 and 1 respectively. The axial force due to the nacelle self-weight is 1067.33 kN and the corresponding compressive

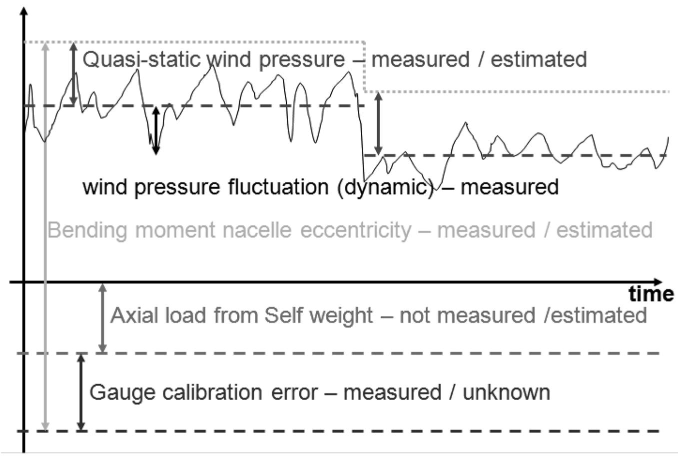

Fig. 5 Strain history at an arbitrary location and its decomposition in static or quasi-static components and dynamic component

stresses at the same levels are, respectively, 3.11 MPa and 3.87 MPa.

The component representing the gauge calibration error in Fig. 5 is included in the measured values. Since it is unknown, it must be dropped out from the measurement results zeroing the system during very low wind speed conditions, as it was explained above. This was done before starting monitoring under a mean wind speed of 4.62 m/s, a mean wind direction of 170ºC. measured clockwise from North (see Table 2) and a mean temperature of 13.7ºC.

Added to these two time invariant strain components, there are the strains varying in time due to nacelle position and due to wind pressure. Considering the first one, it refers to the bending moment effect due to the nacelle self-weight eccentricity relatively to tower axis (0.725 m). The maximum vertical stress in the shell at level 0 due to this bending moment effect is numerically estimated as being 2.15 MPa. However, for a given measurement point this effect varies during operation, since it depends on the nacelle orientation. In order to have the correct effect of the nacelle azimuth in the measured signals, the calibration was made using the mean values of twelve time series of the signals measured for nacelle positions varying from azimuth 0º to 360º with increments of 20º and observing the wind and temperature conditions mentioned above.

The final result of the calibration is to assure that the measurements related to strains accurately represent the static and dynamic effect of wind pressure on the turbine blades and on the tower including the effect of bending moment produced by the nacelle eccentricity. For instance, to compute the final stresses including static non measured axial force at levels 0 and 1 the values 6.67 MPa and 6.56 MPa, respectively, must be added as uniform compressive vertical stresses in the shell.

5. Strain measurements

5.1 Wind induced stresses in the shell

Stresses in the shell are obtained from the strain measurements using a Young's modulus given by E = 200 GPa. Three stress components can be obtained at each measurement point. The principal stresses can be estimated using the following expressions

$$\begin{Bmatrix} \sigma_1 \\ \sigma_2 \end{Bmatrix} = \frac{\sigma_x + \sigma_y}{2} \begin{Bmatrix} + \\ - \end{Bmatrix} \sqrt{\left(\frac{\sigma_x - \sigma_y}{2}\right)^2 + \tau_{xy}^2} \qquad (1)$$

where σ_x is the horizontal stress, σ_y is the vertical stress and τ_{xy} is obtained from Eq. (2)

$$\sigma_\theta = \frac{\sigma_x + \sigma_y}{2} + \frac{\sigma_x - \sigma_y}{2}\cos 2\theta + \tau_{xy}.sin2\theta \qquad (2)$$

taking θ as 45º and σ_θ as the stress obtained with the inclined strain gauge.

The results shown in this section were obtained during the initial period of test measurements after calibration was performed. During this period there were interruptions due to difficulties in data transmission, malfunction of the monitoring system and maintenance works in the tower. Most

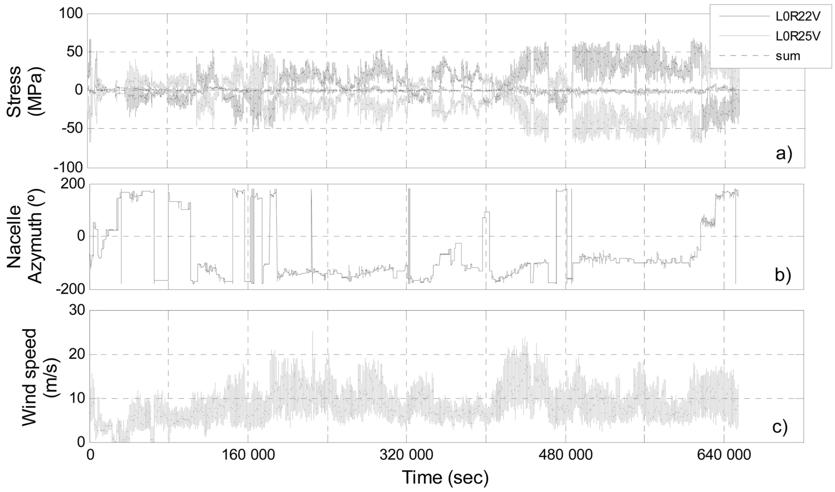

Fig. 6 Typical time histories: (a) vertical stress at points L0R22V and L0R25V and respective sum, (b) nacelle azimuth – positive clockwise from North direction and (c) wind speed at nacelle level

of the records were started manually using remote access to the acquisition software or even locally. Fig. 6 shows a set of time histories obtained during a certain period of operation put sequentially in time without the real time gaps. Fig. 6(a) shows the vertical stress at two diametrical opposite measurement points located in the shell at level 0–L0R22V and L0R25V (see Table 2 for location). Values are plotted every 0.4 seconds corresponding to the acquisition rate of 2.5 Hz. The additional subplot representing the vector sum of those signals shows an acceptable level of noise with a RMS equal to about 7% of the signal's RMS. The stress evolution is consistent with the nacelle direction represented in Fig. 6(b) and with the wind speed (Fig. 6(c)). It is noted that the stresses are relatively low and the nacelle azimuth changes frequently during an initial long period, probably due to the fact that most of the records were started manually. The instantaneous extreme and average values of vertical stresses at level 0 and of the wind velocity measured during this period are given in Table 3. The extreme values must not coincide with the real maximum vertical stresses in the shell but should be very close to them. Adding the compression from self-weight a maximum compressive stress of about 80 MPa can be estimated.

5.2 Wind induced stresses in the bolts

The bolts in the connections are pre-stressed and therefore the stresses induced by operation are

Table 3 Vertical stresses in the shell during the testing period for which wind speed maximum was 25 m/s and average was 8.3 m/s.

	Vertical stress (MPa)			
	L0R22V	L0R23V	L0R24V	L0R25V
Maximum	67.1	62.2	65.6	62.7
Minimum	–61.8	–72.7	–71.8	–71.3
Average	10.7	–13.2	–24.0	–11.0

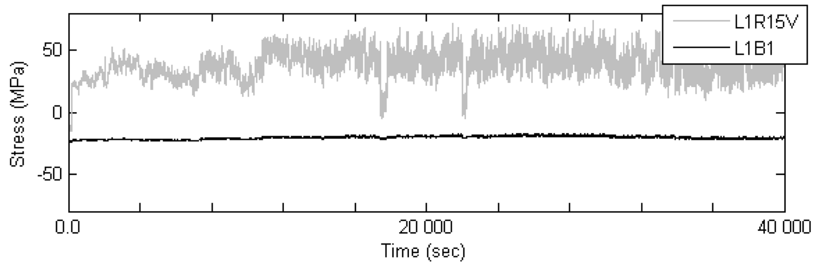

Fig. 7 Comparison between bolt stresses and shell vertical stresses at level 1

expected to be much smaller than those in the shell. For the sake of comparison, at level 1 the external diameter of tube is 3917 mm, the shell thickness is 20 mm and the flange thickness is 175 mm. Considering that the contact between flanges is perfect the ratio between vertical stresses in the shell and in the flange due to a bending moment is proportional to the inertia ratio at both section levels, which is about eight.

Fig. 7 shows a comparison of stress histories measured in bolts and shell at level 1. The coefficient of variation (standard deviation divided by the mean value) of stress in the bolt is about five times smaller than in the shell. The mean value of about 20 MPa represented as compression in the bolt corresponds to the pre-stress losses experimented by the bolt since the calibration of measurement system was completed.

6. Acceleration measurements and modal identification

6.1 Modal extraction from measurements

After erection of the tower and before operation starts a preliminary modal identification was performed. The methodology used relies on output-only methods and ambient vibration response analysis (Bendat and Piersol 1993, Brinker *et al*. 2000, Kelly 2000). The three accelerometers at the top of the tower (level 3) and two at each of the levels 1 and 2 were used. The acceleration measurements for modal extraction were made during the idle state of the turbine.

A methodology in the frequency domain was used to identify the modal parameters, which consists of simply picking the peaks of the spectral estimates of the measured signals to identify the natural frequencies. The Enhanced Frequency Domain Decomposition (*EFDD*) (Brinker *et al*. 2000) implemented in a software package for system identification (SVS 2007) was used to extract the modal information from the ambient free vibration. The corresponding average of the normalized singular values of the spectral density matrices are shown in Fig. 8. The marked peaks correspond to four flexural mode shapes of the tower, two bending modes in x and y directions. Table 4 summarizes the obtained results for the modal parameters. Some difference may be expected between the fore-aft and the side-to-side natural frequencies of the tower. However, it is to be noted that the accuracy of the measurements tends to be of the same order of that difference.

The viscous damping identified in the first and second mode is higher than expected for this type of structure. Since the measurements were made during relatively strong wind, the aero elastic damping induced by the interaction with the wind is probably the cause for the increase of the damping ratio.

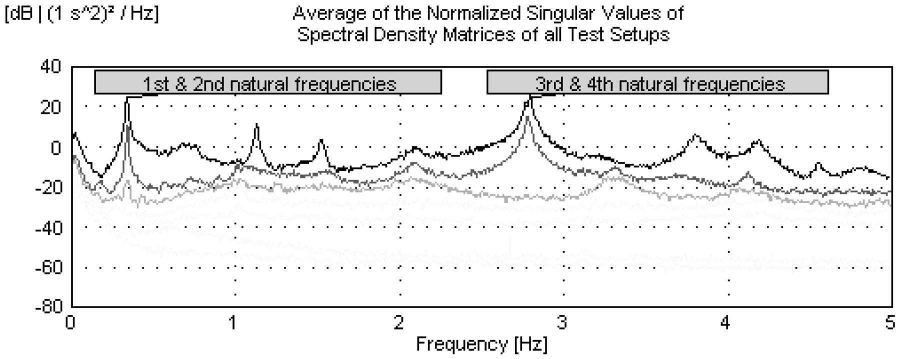

Fig. 8 Singular values of the spectral density matrices

6.2 Finite element model identification

To carry out the structural identification of the tower a finite element model was developed in the software *LUSAS* (*LUSAS*, v14a, b) using quadratic thick shell elements with 8 nodes. The shell elements divided the tower in 80 parts along the height and 24 along the perimeter according to the geometry given in Table 1 (Lavassas *et al.* 2003). The reinforced concrete foundation and the interaction with soil foundation were also included in the model. The plan view of the foundation is an octagon inscribed in a circle of 17 m diameter. The thickness varies between 0.95 m at the border up to 2.5 m in the center. The *FE* model uses 3D solid continuum finite elements for the concrete foundation and linear springs for the contact with the soil.

The model parameters used for model updating were: i) the mass of the tower, ii) the stiffness of the springs simulating the soil-structure interaction and iii) the vertical eccentricity of the turbine's centre of gravity.

Concerning the mass of the tower, all the interior elements of the tower as cables, platforms, ladders, elevator and ancillary equipment had to be considered in the global mass. A sensitive analysis studying the effect of increasing up to 15% the original mass of the tower was carried out. The results are shown in Fig. 9(a) where the percentage of deviation of each calculated natural frequency from the corresponding measured one is plotted against the percentage of added mass to the original mass of the steel tower with nacelle. The influence of changing mass is higher for the higher natural frequencies.

The second parameter was varied around the reference soil subgrade coefficient that was obtained in the soil tests. Depending on the modulus of elasticity of the soil, E_s, the springs' stiffness is based on the subgrade reaction coefficient k_z defined according to the following expression (Bowles 1988, Adhikari and Bhattacharya 2011)

$$k_z = \frac{E_s}{B(1-\upsilon_s^2)}[kN/m^3] \tag{3}$$

where B is the diameter of the foundation and n_s is the poisson coefficient of the soil. The stiffness of each uniaxial spring modelled under the foundation is obtained multiplying the influence area of each spring by k_z. To calibrate the *FE* model E_s was considered to vary between 150 MPa and 300 MPa. The influence of this parameter on the results is shown in Fig. 9(b).

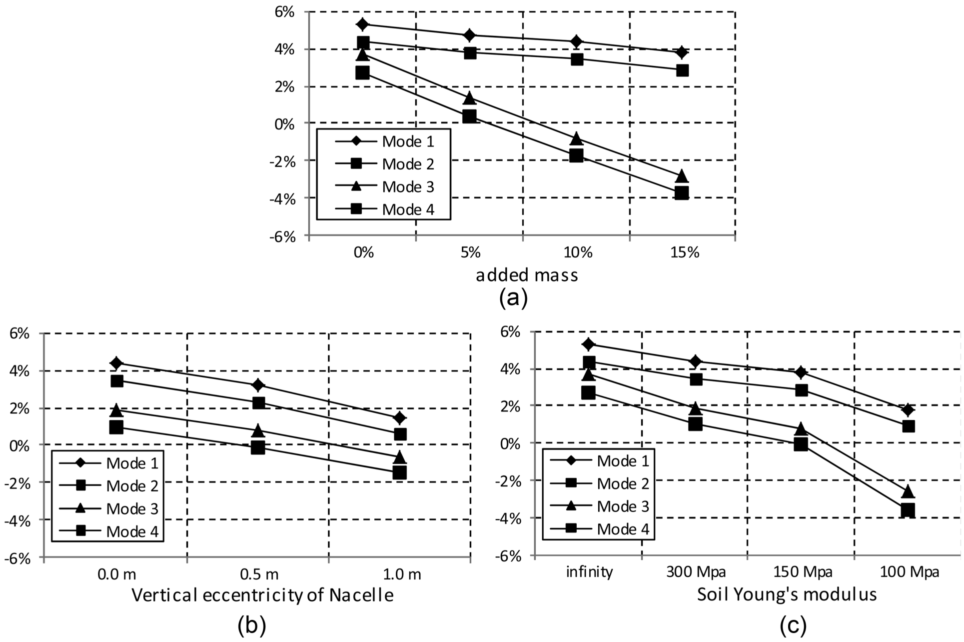

Fig. 9 Deviation of the natural frequencies in the FE model from measured results when varying: (a) mass, (b) soil stiffness and (c) vertical eccentricity of nacelle

Table 4 Natural frequencies, modes and damping

		Mode			
		1	**2**	**3**	**4**
Frequency (Hz)	Measured	0.340	0.343	2.767	2.794
	Updated *FE* model (*Es* = 300 MPa; *e* = 1.0 m)	0.345	0.345	2.751	2.751
Damping **(%)**		1.32	0.96	0.13	0.23
Mode type		Bending Nacelle direction (*x-x*) 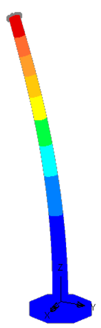	Bending Transversal to Nacelle direction (*y-y*) 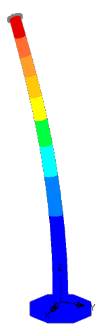	Bending Nacelle direction (*x-x*) 	Bending Transversal to Nacelle direction (*y-y*) 

Concerning the vertical eccentricity of the nacelle, the reason for including it was that the exact value of the eccentricity was not given in the design documents of the wind tower. Its influence in the frequency values is shown in Fig. 9(c) for an eccentricity varying from 0 m to 1.0 m. The final model considers $E_s = 300$ MPa and 1.0 m vertical eccentricity for the centre of gravity of the nacelle relative to the top of the steel tower. Results for the natural frequencies and mode shapes are shown in Table 4.

7. Conclusions

The main objective of the research is to improve competitiveness of steel towers used to support multi mega-watt wind turbines. A better knowledge of the real load distribution along the tower height and the stress distribution nearby the steel connections will help to review stability issues related to more slender shell and detailing such as door openings and number and stiffness of stiffening rings.

The monitoring system developed for the current steel tower aims to allow the updating and calibration of advanced *FE* models, which can be used to improve next generation of steel wind towers. The paper presents the experimental program concerning the instrumentation and the calibration of equipment used for monitoring of a 80 meters high steel wind tower supporting a 2.1 MW turbine Wind Class III IEC2a erected in the central part of Portugal.

The monitoring system installed is able to measure strains in three directions of 26 points of the inner surface of the tower shell and in 18 pre-stressed bolts. Additionally, accelerations in three levels of the tower, inclinations at two levels and the inner temperature are measured. Calibration of the equipment was performed and preliminary measurements were used for consistency analysis of the data. A finite element model was developed and updated through modal identification performed before the turbine started production. The *FE* model is intended to serve as a computational tool for interpretation of measurement results and identification of possible changes in the dynamic response of the tower during its service life.

A comprehensive set of results obtained during the first year of monitoring is reported in the second part of this paper (Rebelo 2011).

Acknowledgements

The authors are grateful for the financial support of the RFCS (Research Fund for Coal and Steel of the European Community) under the contract RFSR-CT-2006-00031 and for the very good collaboration with the other project partners: RWTH (Aachen, Germany), Germanischer Lloyd Industrial Services GmbH (Hamburg, Germany), Aristotle University of Thessaloniki (Thessaloniki, Greece), Repower Portugal Equipamentos Eólicos SA (Oliveira de Frades, Portugal) and Rautaruukki Oyj (Hämeenlinna, Finland). The collaboration of all project partners and specially Repower Portugal is warmly thanked. Furthermore, the authors thank Eng. Fernando Leite (CONTROLAR, Portugal) and Eng. José Saraiva (Repower Portugal) for their support to development of the software application and to the instrumentation works.

References

Adams, D., White, J., Rumsey, M. and Farrar, C. (2011), *Structural health monitoring of wind turbines:method and application to a HAWT*, Wind Energ., Published online in Wiley Online Library.

Adhikari, S. and Bhattacharya, S. (2011), "Vibrations of wind-turbines considering soil-structure interaction", *Wind Struct*., **14**(2), 85-112.

Bendat, J.S, and Piersol, A.G. (1993), *Engineering application of correlation and spectral analysis*, John Wiley & Sons.

Bowles, J.E.(1988), *Foundation analysis and design*, McGraw-Hill.

Brinker, R., Zhang, L. and Andersen, P. (2000), "Modal identification from ambient response using frequency domain decomposition", *Proceedings of the IMAC 18, the international Modal Analysis Conference*, San Antonio, TX, USA

Burton, T., Sharpe, D., Jenkins, N. and Bossanyi, E. (2001), *Wind energy handbook*, John Wiley & Sons.

Chou, Jui Sheng and Tu, Wan Ting (2011), "Failure analysis and risk management of a collapsed large wind turbine tower", *Eng. Fail. Anal*., **18**(1), 295-313.

CEN (2005), "EN 1993-1-9: Design of steel structures - Part 1-9: Fatigue", Brussels.

Dally, J.W., Riley, W.F. and McConnell, K.G. (1993), *Instrumentation for engineering measurements*, 2nd Ed., John Wiley & Sons.

Hau, E. (2006), *Wind Turbines: fundamentals, technologies, application, economics*, Springer, Berlin.

Kelly, S.G. (2000), *Fundamentals of mechanical vibrations*, 2nd Ed., McGraw-Hill international.

Lavassas, I., Nikolaidis, G., Zervas, P., Efthimiou, E., Doudoumis, I.N. and Baniotopoulos, C.C. (2003), "Analysis and design of the prototype of a steel 1-MW wind turbine tower", *Eng. Struct*., **25**(8), 1097-1106.

LUSAS, Element Reference Manual – version 14a, UK.

LUSAS, Modeller Reference Manual – version 14b, UK.

NI-National Instruments (2006), "Labview full development system", version 8.2.

Rebelo, C., Veljkovic, M., Matos, R. and Simões da Silva, L. (2011), "Structural monitoring of a wind turbine steel tower - Part II: monitoring results", *Wind Struct.,*

SVS (2007), *ARTeMIS Extractor pro*, release 4.1, Structural Vibration Solutions, Aalborg, Denmark,

Swartz, R., Lynch, J.P., Zerbst, S., Sweetman, B. and Rolfes, R. (2010), "Structural monitoring of wind turbines using wireless sensor networks", *Smart Struct. Syst*., **6**(3), 183-196.

Veljkovic, M. *et al*. (2012a), *High-strength tower in steel for wind turbine*, Final Report, RFSR-CT-2006- 00031. Brussels: RFCS publications, European Commission.

Veljkovic, M. *et al*. (2010b) "Friction connection in tubular towers for wind turbines", *Stahlbau*, **79**(9), 660-668.

Veljkovic, M. *et al*. (2011), *Wind turbine tower design, erection and maintenance*, in Wind energy systems: *Optimising design and construction for safe and reliable operation* (Ed. J.D. Sørensen), Aalborg University and J N Sørensen, Technical University of Denmark, Denmark, Woodhead Publishing Limited, Cambridge, UK.

CC